Open Access

OBM Genetics

Original Research

Synergistic Effect of Resveratrol and Paclitaxel in the Treatment of Malignant Pleural Mesothelioma

Lunawati Lo Bennett *

College of Pharmacy, Union University, 1050 Union University Dr, Jackson, TN 38305, USA; E-Mail: llbennett@uu.edu

* **Correspondence:** Lunawati Lo Bennett; E-Mail: llbennett@uu.edu

Academic Editor: Fabrizio Stasolla

Special Issue: Cancer Genetics and Epigenetics Alterations II

OBM Genetics
2024, volume 8, issue 4
doi:10.21926/obm.genet.2404268

Received: June 11, 2024
Accepted: October 16, 2024
Published: October 18, 2024

Abstract

Malignant pleural mesothelioma (MPM) is a lethal and aggressive cancer due to exposure to asbestos since this carcinogen is still being used in industrial buildings and housing in several countries. Untreated MPM has a median survival time of 12 months, and most people die within 24 months after diagnosis. If caught early, surgery may be performed. Treatment option for palliative care is limited using platinum with pemetrexed. Malignant transformation of a cell is attributed to a series of genetic and epigenetic events involving alterations in several oncogenes, tumor suppressor genes, and others. Different anticancer and antioxidants with anticancer properties were tested individually and in combination to find the best synergistic effect in killing MSTO-211H, a lung mesothelioma cell line used as model of MPM. Once the combination was identified, assays and staining methods such as MTT, Rhodamine123, Hoechst 33342, Nuclear ID Red/Green, and Western Blot were performed to identify different proteins involved in apoptosis and cell signaling cascade to proof the cytotoxic effect of the combine anticancer and antioxidant treatment. Combination of Paclitaxel (PAC) at 3 µM and Resveratrol (RSV) at 62.5 µM showed synergistic effect on MSTO-211H cells by causing inhibition of epidermal growth factor receptor (EGFR), inhibition of mitogen activated protein kinases (MEKs) 1-4, inhibition of programmed death ligand-1 (PDL-

1), inhibition of cell cycle proteins, and induction of caspases 3-8. This study provided possible potential application of using RSV as a chemo-enhancing compound with PAC in the treatment of MPM.

Keywords
Malignant pleural mesothelioma; lung cancer; paclitaxel; EGFR; MEKs; resveratrol; reactive oxygen species; caspases

1. Introduction

Malignant pleural mesothelioma (MPM) is an exceptionally lethal and aggressive cancer originating in the pleural cavity also impacting the outer lining of the lung [1, 2]. Both genders are equally susceptible to MPM when exposed to asbestos, predominantly through occupational or environmental means, with approximately 80% of reported cases attributed to male workers [3-5]. Asbestos, a group fibrous mineral of 3-4000 products, historically has been utilized in numerous commercial products and non-commercial buildings for centuries. Asbestos harbors carcinogenic fibers, contributing to various cancer [2].

Despite its prohibition use in Western countries, MPM incidence persists in regions where asbestos use remains prevalent, notably in rural or industrialized areas undergoing building renovations with asbestos [5, 6]. However, environmental exposure continues due to human activities disturbing natural asbestos deposits, compounded by residential proximity to asbestos-rich locations like underground rock formations [4]. A significant milestone was achieved on March 19, 2024, as the United States Environmental Protection Agency (EPA) issued a landmark ruling to ban chrysotile asbestos, the sole form of asbestos use in the US [7].

MPM carries a dismal prognosis, with a median survival ranging from 6 to 18 months and a 5-year survival rate of less than 5%. Due to its latency of 20 to 60 years post-exposure to asbestos, patients with MPM are often diagnosed at an advanced stage [4, 8-10]. This bleak outlook is exacerbated by the disease's aggressive nature. Furthermore, it is often compounded by the lack of reliable screening tools, specific biomarkers, and effective systemic therapies [8-10].

Currently, a diagnostic method involving immunohistochemical expression of serine and arginine-rich splicing factor 1 (SRSF1) was tested in a preliminary study. SRSF1 appears to be involved in MPM pathogenesis, and its expression may serve as a useful prognostic biomarker [11]. Additionally, this group of researchers used ATG7 immunohistochemical expression to assess the overall survival (OS) of patients with MPM. A significant correlation between ATG7 expression and the overall survival of patients with MPM was observed, with a mean OS of 12.5 months in patients with high expression versus a mean OS of 4.5 months in patients with low ATG7 expression [12].

MPM affects up to 1.5 million people in the USA annually, some in the form of the accumulation of pleural fluid (MPE), with the majority being MPM. Approximately 3200 new cases of MPM are diagnosed annually in the United States. This leads to significant healthcare resource usage and hospital admissions, with a median stay of 5.5 days in the hospital, causing an estimated $5 billion in healthcare costs per year [13].

Current standard care of MPM includes surgery with intent to cure if early stage of MPM diagnosis is identified or palliative care using combination chemotherapy of platinum such as carboplatin or cisplatin and anti-folates such as pemetrexed [14, 15]. There is no clear evidence to support the use of neo-adjuvant or adjuvant chemotherapy or second or third agents to treat MPM.

Currently, immunotherapy with checkpoint inhibitors targeting programmed death ligand 1 (PD-L1), such as nivolumab, durvalumab, or pembrolizumab, or cytotoxic T-lymphocyte–associated antigen 4 (CTLA-4), such as ipilimumab or tremelimumab, are being tested in phase II or III clinical trials [16, 17]. Any attempt to treat MPM is a very welcoming addition treatment options to this aggressive lethal cancer [18, 19].

Paclitaxel (PAC) is a compound isolated from *taxus brevifolia* that works as anticancer drug by promoting tubulin polymerization and stabilizing microtubules from depolymerizing which causes mitotic arrest and cells death [20, 21]. This taxane has been approved by the Food and Drug Administration (FDA) for the treatment of ovarian, breast, and lung cancers [22].

Resveratrol (RSV), trans-3,4',5-trihydroxystilbene, is a naturally occurring polyphenolic compound found in many foods mostly red grapes which has antioxidant activity and had been studied extensively as a chemo-preventive agent against various types of human cancers. The compound works by inhibiting cancer initiation, promotion, and progression [23, 24].

In the present study, the effects of PAC at the lowest concentration, either individually or in combination with RSV at the appropriate concentration, were analyzed to identify their utility as treatment options for MPM.

2. Materials and Methods

2.1 Cell Culture and Media

MSTO-211H (ATCC), a human MPM cell line used in this study as a model, was cultured in RPMI-1640 media (Corning) supplemented with 10% fetal bovine serum (FBS) and 1% streptomycin/penicillin (ATCC). This cell line exhibited fibroblast morphology that was isolated in 1985 from the lung of a 62-year-old, white male patient with biphasic mesothelioma.

MPM is classified into three major histological subtypes: epithelioid, sarcomatoid, and biphasic, with each subtype exhibiting distinct biological behaviors and treatment responses. The MSTO-211H cell line was selected as a representative model due to its biphasic nature, which consists of both epithelioid and sarcomatoid components. This makes it a valuable model for studying the broader range of biological behaviors seen in MPM, as it encompasses characteristics of both major subtypes. As such, MSTO-211H provides a reasonable prototype for exploring potential treatment strategies for MPM in a cost-effective manner.

The cells were maintained in incubator at 37°C in 5% CO_2 humidified environment. To confirm there is no contamination with mycoplasma and other contaminant, Mycofluor Mycoplasma Detection Kit, and Cell Culture contamination Detection Kit (both from Invitrogen) were used. There was no contamination detected.

2.2 MTT Assay

Cell viability was assessed using the MTT (3-[4,5-dimethylthiazol-2-yl]-2,5-diphenyl-tetrazolium bromide) (Sigma) assay, as previously described [21, 22]. Initially, MTT was employed to determine

the selection of doses that cause death of 50% viable cancer cells when exposed to various anticancer compounds individually, such as afatinib, irinotecan, doxorubicin, sorafenib, etoposide, gemcitabine, capecitabine, vincristine, docetaxel, and paclitaxel. Additionally, various antioxidants, including N-acetyl cysteine, alanine, curcumin, glutathione, and resveratrol, were tested in MSTO-211H cells. Combinations of the lowest anticancer concentrations and antioxidants demonstrating the best synergistic effects were selected for further experiments. Briefly, MSTO-211H cells were plated in a 96-well microplate at a density of 1×10^5 cells/ml and incubated overnight to allow adherence. The cells were then treated with a series of concentrations of resveratrol (RSV) (Sigma), paclitaxel (PAC) (LC Laboratories), or their combination. After 24 hours of incubation at 37°C in 5% CO_2, 50 µl of MTT solution (2 mg/ml) was added to each well, followed by a 4-hour incubation at the same conditions. Subsequently, 150 µl of dimethyl sulfoxide (DMSO)(Amresco) was added to dissolve the violet-blue crystals. Cell viability was measured using a spectrophotometer (Molecular Devices) at an absorbance of 570 nm.

2.3 Morphological Analysis

The alterations in morphology of MSTO-211H cells following treatment with PAC, RSV, or their combination for 0 and 24 hours were captured using an inverted microscope (Motic AE31), as detailed in prior studies [25, 26].

2.4 Wound-Healing Assay

To assess the potential of PAC, RSV, or their combination to inhibit cellular migration, MSTO-211H cells were cultured at a density of 1×10^5 cells/ml in a 12-well dish for 24 hours. Subsequently, a scratch assay was performed using a sterile pipette tip. The migration area was then photographed at 40× magnification using an inverted microscope. The width of the scratch was measured at 0- and 24-hours post-scratch, in accordance with established protocols [25, 26].

2.5 Apoptosis Assay

To observe the nuclear chromatin morphological changes in MSTO-211H cells resulting from treatment with PAC, RSV, or their combination, a NucBlue™ live cell Hoechst 33342 (Life Technologies) staining assay was conducted following established protocols [25, 26]. Subsequently, the quantities of apoptotic and non-apoptotic cells were captured using the Floid Cell Imaging Station (Life Technologies), and fluorescence intensities were measured using Image J software (NIH). A histogram was then prepared to compare the percentage changes of apoptotic cells among the different treatment groups.

2.6 Mitochondrial Membrane Potential (ψ_m) Assay

To determine alterations in mitochondrial membrane potential, cells were stained with the Rhodamine 123 fluorescence probe (Sigma) following established procedures [25, 26]. Subsequently, the relative intensities of green fluorescence were captured using FLoid cell imaging.

2.7 Intracellular ROS Assay

To compare intracellular ROS generation in MSTO-211H cells following individual treatment with PAC, RSV, or their combination, an H2DCF-DA (2',7'-dichlorodihydrofluorescein diacetate) (Invitrogen) staining assay was conducted according to the manufacturer's protocol (Invitrogen), as previously reported [25, 26]. The relative intensities were then captured using the Floid Cell Imaging Station.

2.8 Live and Death Cells Assay

To assess alterations in the deoxynucleic acid (DNA) of MSTO-211H cells resulting from treatment with PAC, RSV, or their combination, a Nuclear-ID Red/Green cell viability assay was conducted following the manufacturer's protocol (Invitrogen), as previously described [26]. This assay utilizes a simultaneous combination of red and green dyes to distinguish live and dead cells, which were captured using the Floid Cell Imaging System. Subsequently, a histogram was prepared to compare the quantities of live and dead cells using Image J software.

2.9 Western Blot Analysis

Western blot analysis was conducted to assess changes in the levels of key proteins following treatment of MSTO-211H cells with PAC, RSV, or their combinations, in accordance with established procedures [23, 24]. Briefly, proteins were extracted from cells using RIPA buffer supplemented with protease and phosphatase inhibitors (Sigma), and their concentrations were determined using the Bradford protein assay following the manufacturer's protocol (BioRad Laboratories). Equal amounts of 50 µg proteins were then loaded onto 10% polyacrylamide gels and separated via electrophoresis. Subsequently, the proteins were transferred onto Immuno-Blot PVDF membranes using the Trans Blot Turbo system (BioRad Laboratories) for 30 minutes. The membranes were blocked for 2 hours in 5% dry milk (Santa Cruz Biotechnology) dissolved in Tris-buffered saline containing 0.1% Tween-20 (TBST) at room temperature. Following blocking, the membranes were incubated overnight with specific primary antibodies. The next day, the membranes were washed several times in TBST and then incubated for 2 hours with secondary antibodies. Primary antibodies Casp-3, -7, -8. -9, cyclin D1, cyclin B1, cytochrome C, PDL1, and AIF-1 (Cell Signaling Technology). Other antibodies β-actin, Bax, Bcl2, CDK7, EGFR, and MEK-1, -2, -3, -4 (Santa Cruz Biotechnology). Protein bands were visualized using Enhanced Chemiluminescence (ECL) (BioRad) Western blotting detection reagents, and images of the bands were captured using the Bio-Rad ChemiDoc XRS+ imaging system.

2.10 Colony Formation Assay

To evaluate the ability of a cell to proliferate indefinitely and form a large colony or clone, 1000 viable MSTO cells were plated in a 24-well plate, followed by treatment with PAC, RSV, or their combination for 1 day as described previously [27]. The media were removed the next day and replaced with fresh media. The cells were then incubated for 10-14 days in 5% CO_2 at 37°C. Subsequently, the cells were fixed with methanol for 15 minutes, followed by staining with 0.05% crystal violet diluted in DPBS for 15 minutes. After washing with DPBS, the stained colonies were photographed.

2.11 Statistical Analysis

Statistical results were expressed as the mean ± SD of three independent sets of experiments. Differences between individual and combination treatment groups were assessed using Newman-Keuls one-way ANOVA. Significance levels were defined as follows: * $P < 0.05$, ** $P < 0.01$, and *** $P < 0.001$.

3. Results

3.1 Cells Viability and Selection of Doses

MTT assay results demonstrated that both Paclitaxel (PAC) and Resveratrol (RSV) reduced the viability of MSTO-211H cells in a dose-dependent manner. Initially, individual anticancer agents, including Sorafenib, Doxorubicin, Etoposide, Gemcitabine, and PAC, were tested at concentrations ranging from 0 to 100 µM to determine their cytotoxic effects (EC50). Similarly, antioxidants such as Vitamin C, Curcumin, Alpha-Lipoic Acid, and RSV were tested individually across a concentration range of 0 to 1000 µM. Of the anticancer agents, PAC exhibited the lowest EC50 at 3 µM. The combination of RSV at 62.5 µM and PAC at 3 µM showed the strongest synergistic effect. Figures 1(A) and 1(B) illustrate cell viability after 24- and 48-hour treatments with serial PAC concentrations (0–100 µM), while Figures 1(C) and 1(D) depict cell viability after treatment with PAC (3 µM) combined with serial RSV concentrations (0–1000 µM) compared to RSV alone.

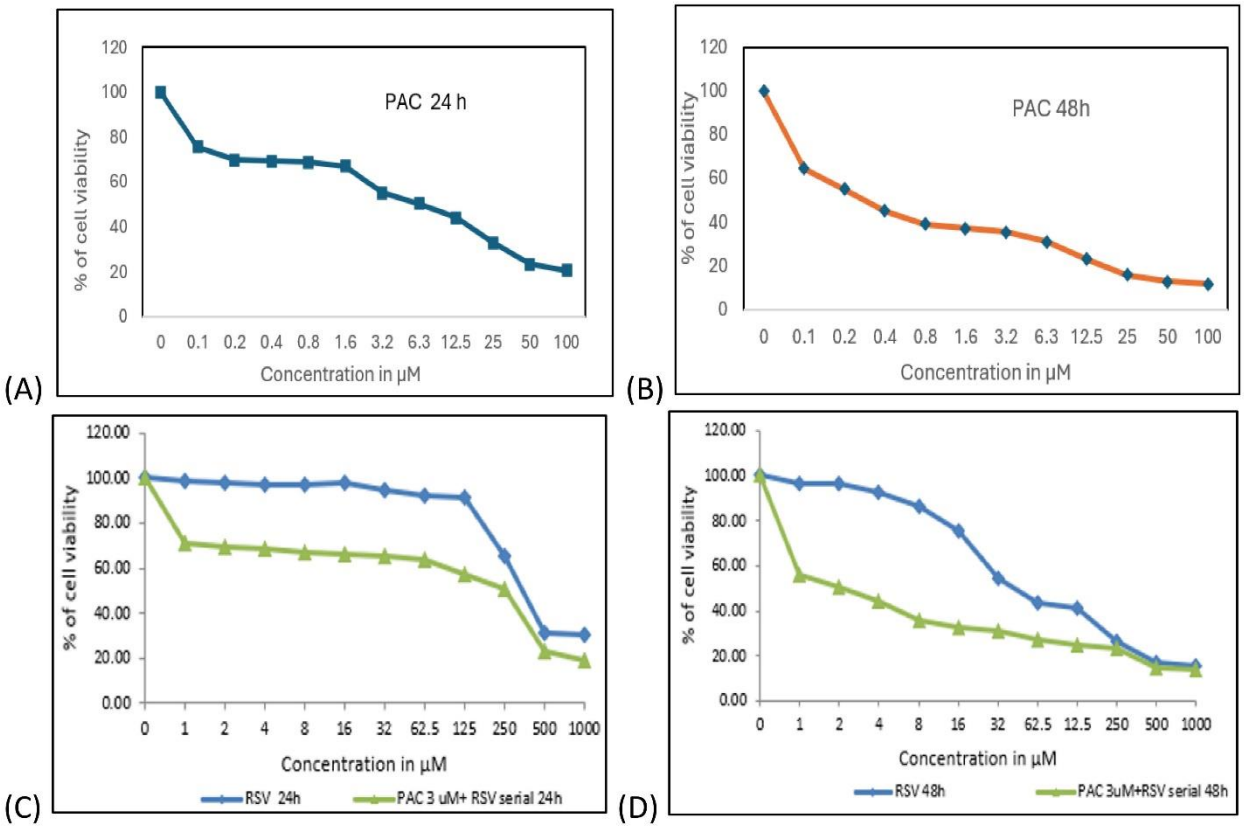

Figure 1 (A) and (B). MTT assay of MSTO-211H cell viability treated with serial concentration of paclitaxel (PAC) for 24 hr or 48 hr. (C) and (D). MTT result using PAC 3

µM and RSV at serial concentration from 0-1000 µM for 24 hr and 48 hr. versus cells treated by RSV only using serial concentration for 24 hr or 48 hr.

3.2 Changed in Cell Morphology

The morphology of cells was altered in all treatment groups compared to the control. In Figure 2, healthy control cells exhibited fibroblast-like growth, adhering to the culture dish, whereas cells treated with a combination of PAC and RSV demonstrated extensive cell death, with most cells floating in the media. Treatment with PAC alone or in combination with RSV resulted in changes in cell morphology after 24 hours of treatment.

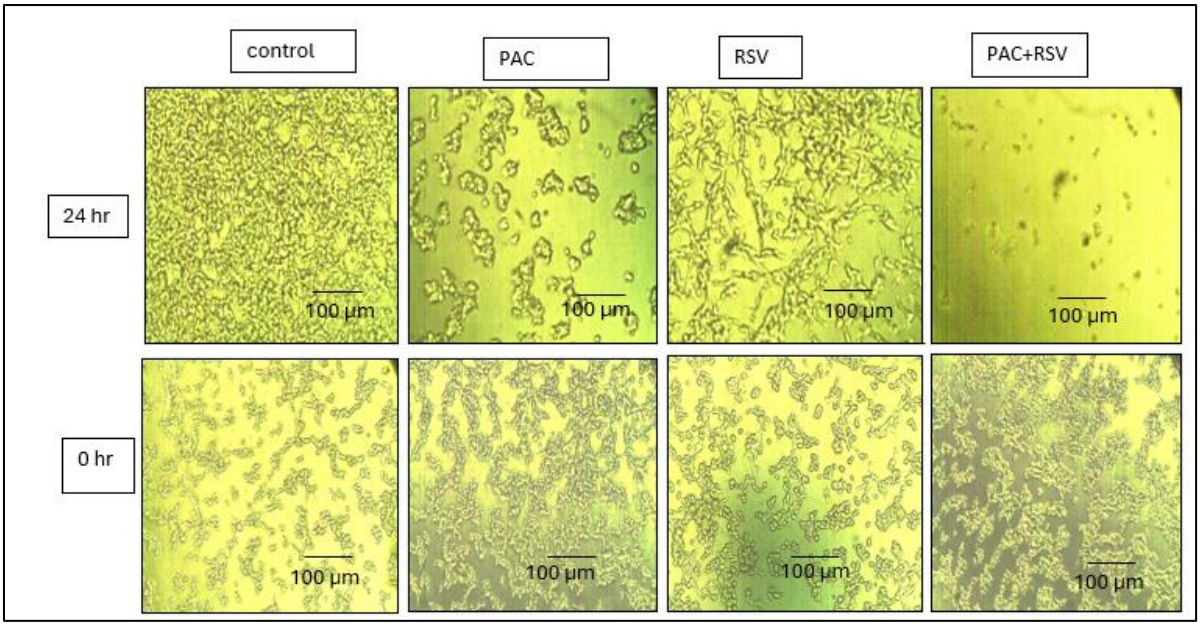

Figure 2 Inverted microscopic images of MSTO-211H after 24 h treatment with PAC 3 µM, RSV 62.5 µM or combination of PAC and RSV. Combination of PAC and RSV caused almost all cells death, detaching from the flask. Scale bar indicated 100 µm.

3.3 Changed in Cell Migration

After 24 hours of treatment, the combination of PAC and RSV induced a significant decrease in cell viability, with nearly all cells dying compared to the control group. In the control group, MSTO-211H cells exhibited substantial migration, almost completely covering the culture dish within 24 hours, indicative of the initial steps in cancer metastasis for MSTO-211 cells. Treatment with RSV alone resulted in a notably slower migration of cells compared to the control as shown in Figure 3.

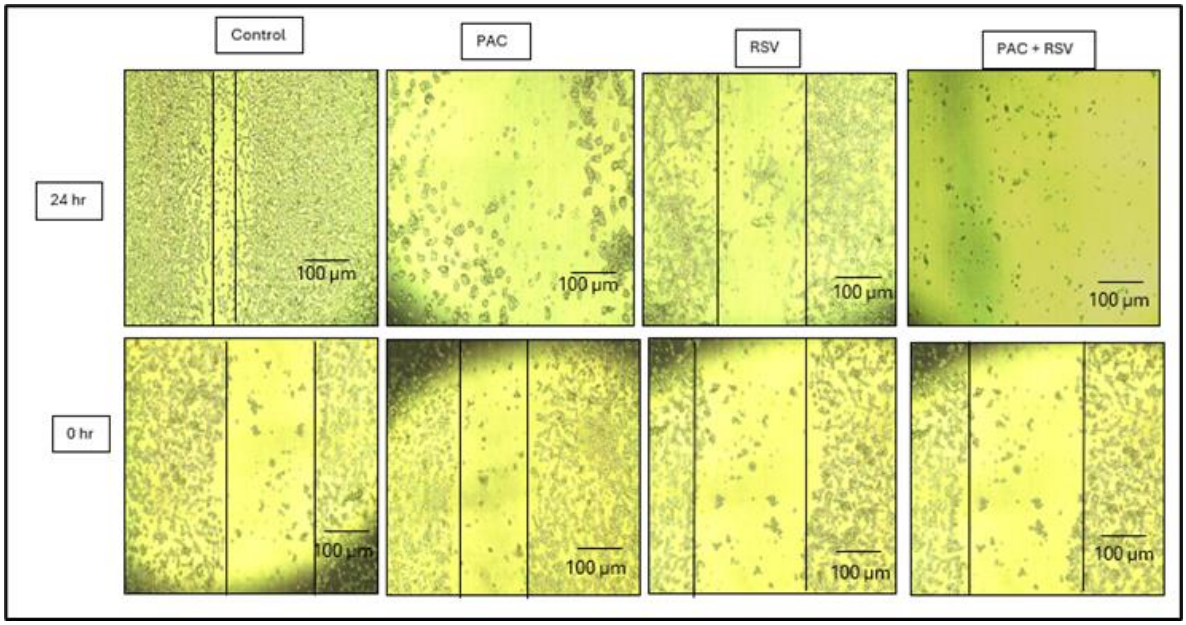

Figure 3 Inverted microscope images of cell migration assay of MSTO-211H after 24 h treatment with PAC 3 µM, RSV 62.5 µM or combination of PAC and RSV. Control cells migrated back after 24 hr, but combination PAC and RSV caused almost complete cell deaths. Scale bar indicated 100 µm.

3.4 Induction of Apoptosis

The combination of PAC and RSV treatment induced more apoptosis than PAC or RSV alone, as detected using the Hoechst 33342 staining method. Apoptotic cells exhibited a bright blue color due to condensed and fragmented nuclei, while control cells showed lower fluorescence intensity, indicating normal and healthy cells (Figure 4(A)). Figure 4(B) displays a histogram comparing apoptotic and non-apoptotic cells, analyzed using Image J software.

Furthermore, Western blot analysis showed changes in the expression of pro-apoptotic Bax and anti-apoptotic BCl2 proteins suggested intracellular ROS generation. The ratio of Bax/BCl2 was slightly higher in cells treated with RSV or in cells treated with combination of PAC and RSV as compared to control cells (1.01 for RSV and 1.04 for combo vs.0.97 control). ROS generation also led to a reduction in mitochondrial membrane potential, resulting in increased release of cytochrome C into the cytosol, further inducing apoptosis. A significant increase in cytochrome C was observed in cells treated with the combination of PAC and RSV (Figure 4(C)). Figure 4(D) displays the histogram depicting cells treated with PAC, RSV, or a combination of PAC and RSV.

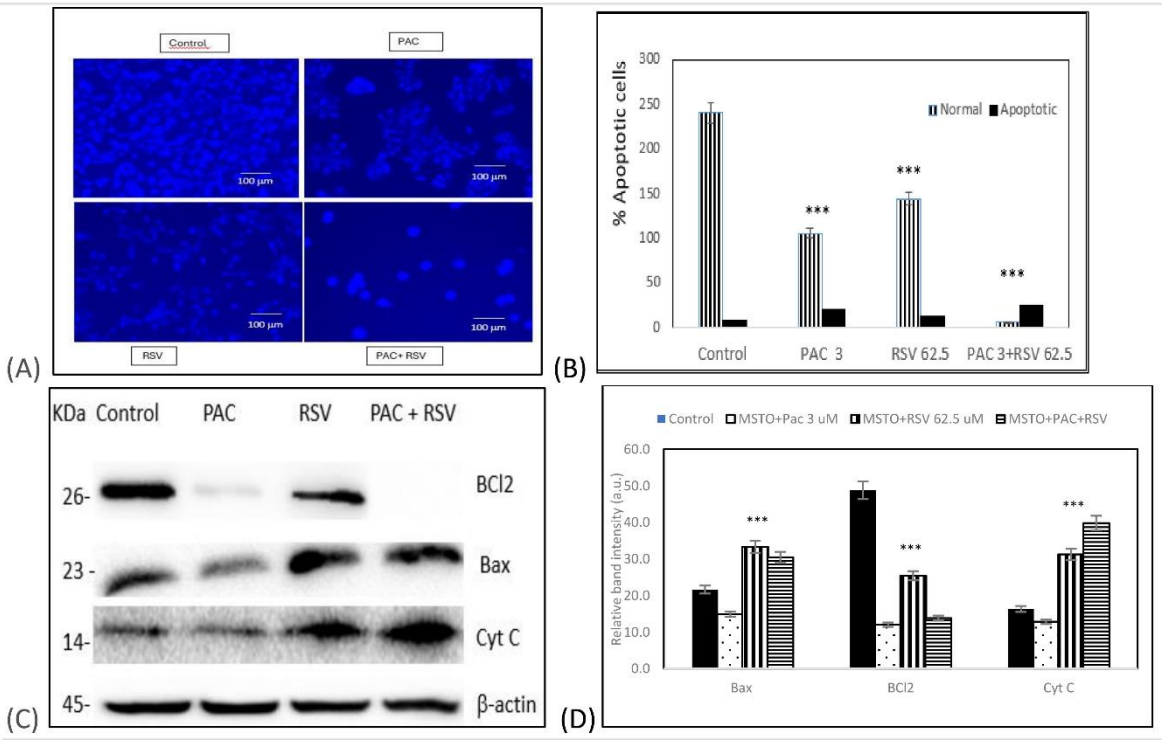

Figure 4 (A) Fluorescence microscopic images of cells after 24 h stained with Hoechst 33342. Bright nuclei indicated apoptotic cells. Histogram in (B) represented the percentage of apoptotic cells and normal cells from different treatment groups comparing to control. ***p < 0.001, post hoc Newman-Keuls test. (C) Western blot analysis data showed expression of Bax, BCl2, and cytochrome C after treatment of cells with PAC, RSV, or combination of PAC and RSV. (D) showed slight change in the ratio of pro-apoptotic Bax/anti-apoptotic BCl2 in cells treated with combination of PAC and RSV (ratio of Bax/Bcl2 in PAC, RSV or combination were 0.96, 1.01, 1.04 respectively vs. 0.97 of the control). Significant increased in cytochrome C was observed in combination group comparing to control. *** p < 0.001, post hoc Newman-Keuls test.

3.5 Depletion Mitochondrial Membrane Potential (ψ_m)

Depletion of mitochondrial membrane potential, indicative of cell death, was identified by the generation of reactive oxygen species (ROS), observed in cells treated with individual PAC, RSV, or the combination of PAC and RSV after staining with Rhodamine 123. Figure 5(A) showed control cells exhibiting higher fluorescent intensity, indicating a healthier membrane potential compared to treated cells. The depletion in mitochondrial membrane potential was more pronounced in cells treated with the combination of PAC and RSV, suggesting a synergistic effect between the anticancer agent and the antioxidant.

Furthermore, Western blot analysis confirmed the depletion of mitochondrial membrane potential showing increase in apoptosis-inducing factor (AIF-1), mitochondrial proteins that mediate caspase-independent cell death. Apoptosis occurred in mitochondria due to several key proteins, such as caspase 3, -7, -8, and -9. The activation of caspases 3, -7, -8, and -9 signifies a crucial event in cancer cell apoptosis. The combination of PAC and RSV indicated a direct role in the activation of initiator caspases (caspase-8 and -9) and executioner caspases (-3 and -7) (Figure 5(B)). Figure 5(C)

illustrates a comparison of the changes in these proteins depicted as a histogram from different treatment groups.

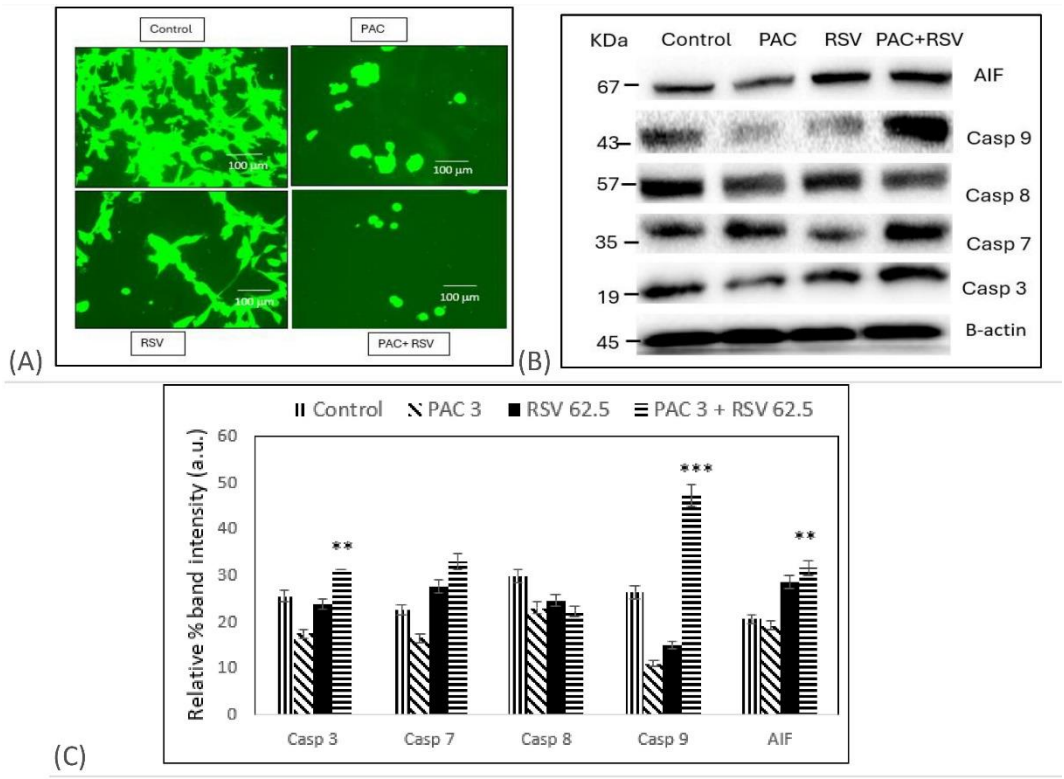

Figure 5 (A) Fluorescence microscopic result from changed in mitochondrial membrane potential (ψ) after cells were staining with Rhodamine 123. Pronounced decreased in mitochondrial membrane potential was observed in combinational cells. Scale bar indicated 100 µm. (B) Western blot analysis from different signaling activity of proteins involved in caspase cascade and AIF-1. (C) showed histogram represents up-regulation of AIF-1 and cas-3, and -9 in cells treated with combination of PAC and RSV comparing to control. ** $p < 0.01$, *** $p < 0.001$, post hoc Newman-Keuls test.

3.6 Intracellular ROS Generation

Intracellular ROS generation was evaluated using the H2DCFDA staining method. Control cells exhibited lower ROS formation, indicated by a darker green intensity, compared to cells treated with PAC or RSV alone. However, cells treated with the combination of PAC and RSV demonstrated the highest intracellular ROS generation, characterized by a brighter green intensity, surpassing both the control and cells treated with PAC or RSV individually as shown in Figure 6.

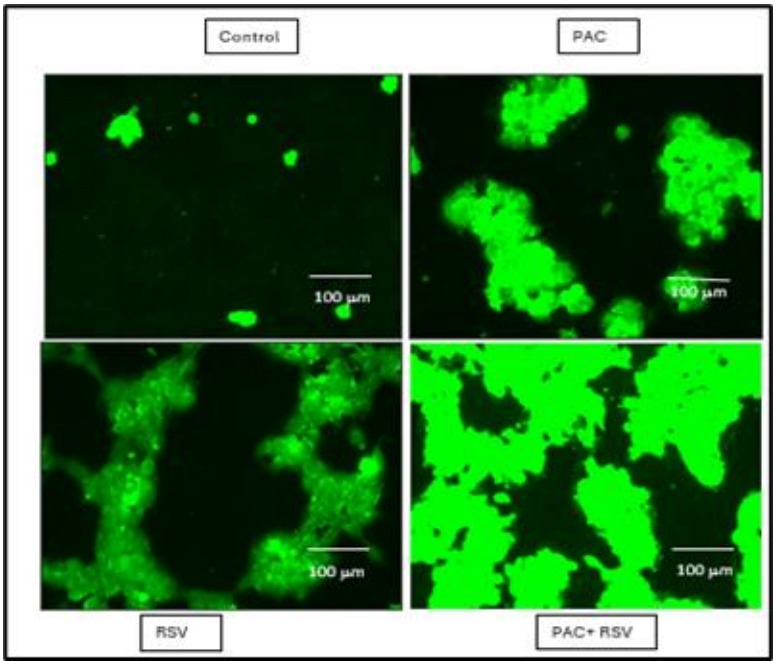

Figure 6 Fluorescence microscopic images of intracellular ROS generated in cells stained with H2DCFDA. Combination of PAC and RSV indicated higher levels of ROS with bright color than PAC or RSV alone. Scale bar indicated 100 µm.

3.7 Increased in Cell Death

The viability of MSTO-211H cells treated with PAC, RSV, or a combination of PAC and RSV was evaluated using the Nuclear-ID Red Green cell staining method. Green fluorescence indicated cells undergoing death, as they were impermeable to the nucleic acid dye, while red fluorescence indicated live cells, which were permeable to the nucleic acid dye. In the control group, cells exhibited a red or orange color when the images from the red and green dyes were merged, indicating cell viability. However, treatment with the combination of PAC and RSV resulted in the highest number of cell deaths, as evidenced by the green or yellow color observed after merging the red and green dyes (Figure 7(A)). Figure 7(B) illustrates the histogram depicting the proportion of dead and alive cells in all groups, as measured using Image J software.

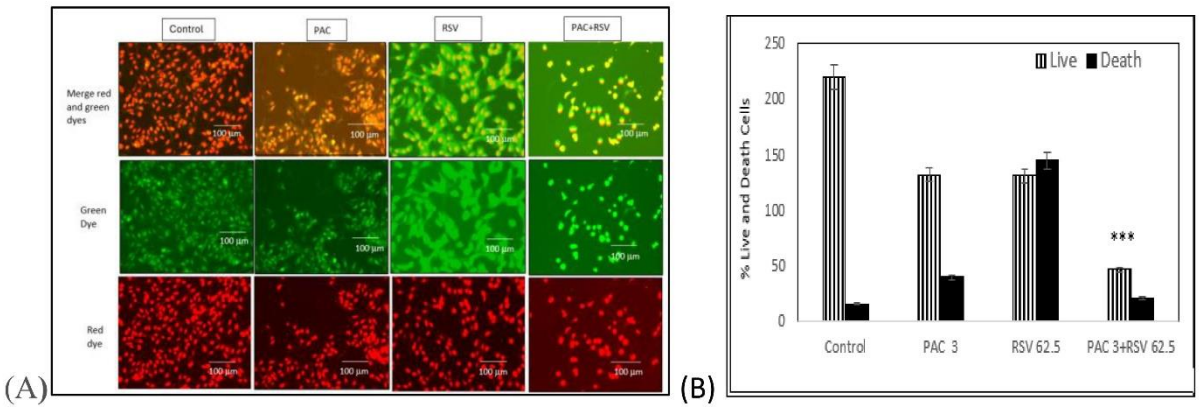

Figure 7 (A) Fluorescence microscopic result from alive and death nucleic acid staining using Nuclear-ID red/green cell viability method. Combination treatment of cells with

PAC and RSV showed significant decreased of alive cells. Scale bar indicated 100 µm. (B) Histogram of different treatment groups comparing death and alive cells comparing to control. *** $p < 0.001$, post hoc Newman-Keuls test.

3.8 Modulation of Cell Cycle Proteins

Inhibition of cell cycle regulatory proteins is considered an important strategy in the treatment of MPM. Western blot analysis revealed a decrease in the band intensity of CDK7, CDK2, cyclin B1, and cyclin D1, which play important roles in cell cycle regulation, in cells treated with the combination of PAC 3 µM and RSV 62.5 µM (Figure 8(A)). Figure 8(B) displays a comparison of the changes in cell cycle proteins depicted as a histogram from different treatment groups.

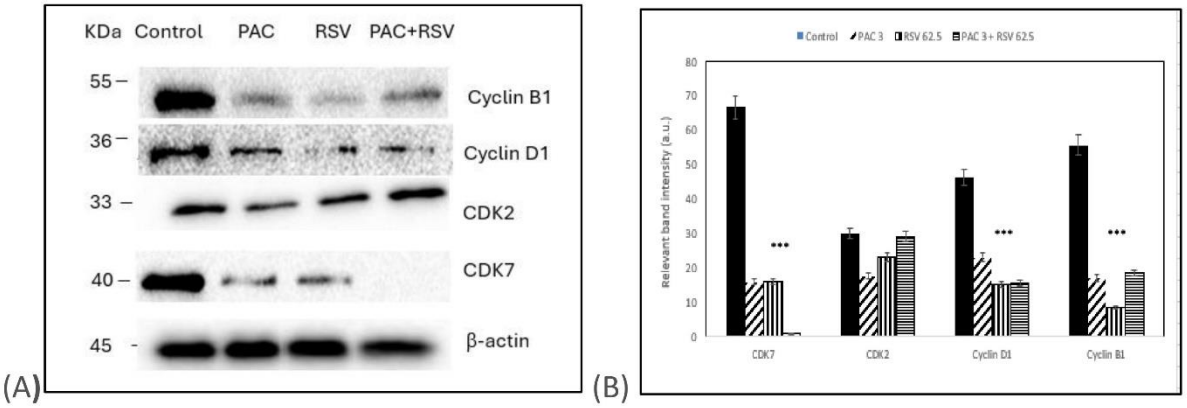

Figure 8 (A) Western blot analysis of proteins involved in cell cycle regulation. The expression of CDK7, cyclin D1 and cyclin B1 significantly decreased in cells treated with combination of PAC and RSV. Slight decreased in CDK2 was noticed. (B) showed histogram down regulation of these proteins comparing to control. *** $p < 0.001$, post hoc Newman-Keuls test.

3.9 Decreased in MEK 1-4 Proteins

Aberrant cell signaling of mitogen-activated protein kinase (MAPKs), along with its active and phosphorylated form, mitogen-activated protein kinases kinase (MEKs), is identified to contribute to cancer progression. Western blot analysis of MEK 1-4 revealed a significant decrease in cells treated with PAC, RSV, or the combination of PAC and RSV compared to the control cells, as depicted in Figure 9(A). Figure 9(B) presents a histogram illustrating the changes in MEK 1-4 proteins across different treatment groups.

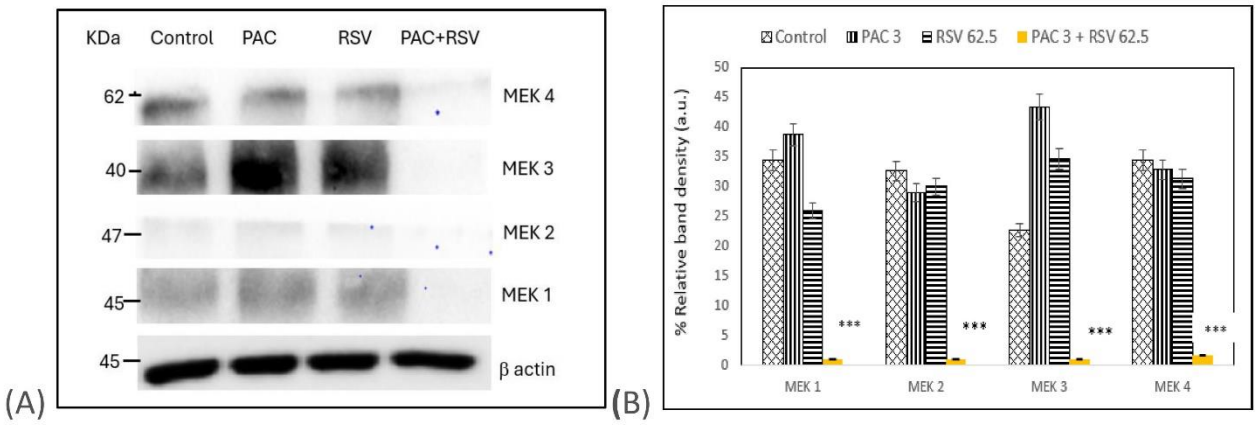

Figure 9 (A) Western blot analysis of MEK-1, -2, -3, and -4 after treatment of cells with PAC, RSV, or their combinations. The expression of these proteins was significantly decrease in cells treated with combination of PAC and RSV. (B) showed histogram expression of these proteins comparing to control. *** $p < 0.001$, post hoc Newman-Keuls test.

3.10 Modulation of EGFR and PDL-1

The epidermal growth factor receptor (EGFR) plays a pivotal role in enhancing cancer growth, invasion, and metastasis. In this study, a combination of PAC and RSV notably reduced EGFR expression in MSTO-211 cells (Figure 10(A)). EGFR activation is known to upregulate programmed death ligand 1 (PDL1). Remarkably, the combination of PAC and RSV also led to decreased expression of PDL1, indicating the cytotoxic effects of this combination therapy through the inhibition of both PDL1 and EGFR. Figure 10(B) illustrates the changes in EGFR and PDL1 expression depicted as a histogram across different treatment groups.

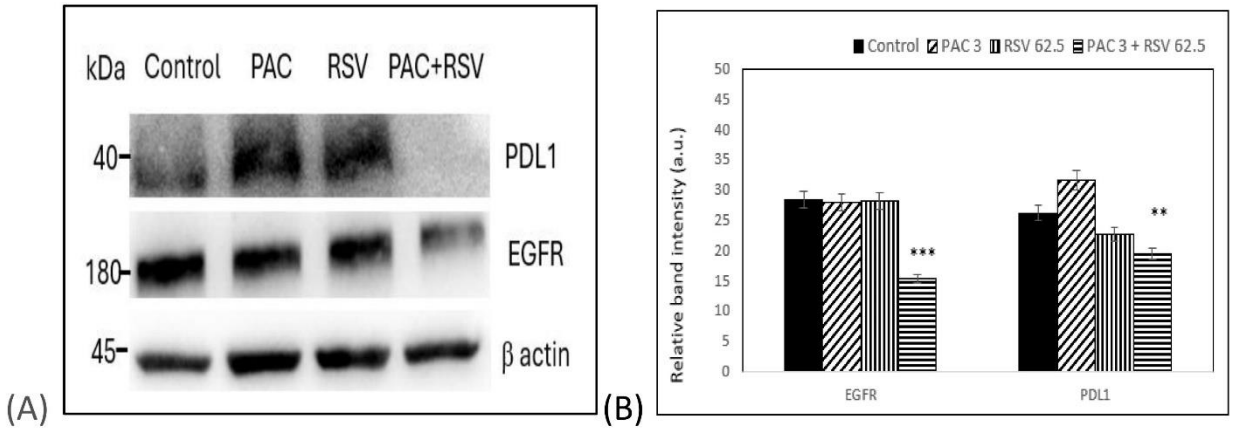

Figure 10 (A) Western blot analysis of EGFR and PDL1 after treatment of cells with PAC, RSV, or their combinations. The expression of these proteins was significantly decrease in cells treated with combination of PAC and RSV. (B) showed histogram expression of these proteins comparing to control. **$p < 0.01$, *** $p < 0.001$, post hoc Newman-Keuls test.

3.11 Decreased in Colony Formation

The impact of PAC, RSV, and their combined treatment on colony formation was studied using microscopy, and the resulting colonies were photographed. A colony, defined as consisting of at least 1000 cells in 24 well-plates, exhibited a decrease in formation with PAC, RSV, or their combination treatments. The lowest number of colonies was observed with the combined treatment, as shown in Figure 11.

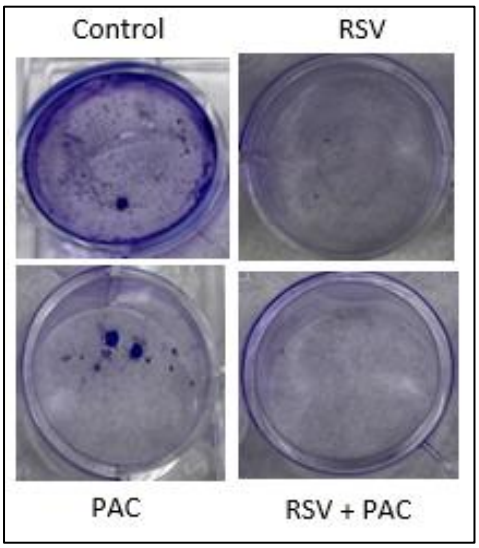

Figure 11 Colony Formation of MSTO cells treated with RSV, PAC, or their combination in comparison to control cells.

4. Discussion

The present study provides convincing evidence that resveratrol (RSV) as an antioxidant has a synergistic effect with lower concentrations of the anticancer agent PAC, leading to cell death in MPM cells. While these two compounds have been studied individually or in combination in various cancer types, to the best of my knowledge, this study is the first to demonstrate the beneficial synergistic effect of combining RSV with PAC in MSTO-211, a model used for MPM cells. A study by Fukui et al. reported that RSV attenuates the anticancer efficacy of PAC in MDA-MB-435 and MDA-MB-231 human breast cancer cell lines but not in MCF-7, another breast cancer cell line. Additionally, RSV didn't attenuate PAC's effect in HepG2 human hepatocellular carcinoma cells, DU-145 human prostate carcinoma cells or MIA-PaCa-2 human pancreas carcinoma cells [28]. They used PAC concentration of 20 nM, while 3 µM was used in this study. Furthermore, Fukui et al.'s study summarized that RSV exerted no protective effect against PAC-induced cell death. However, the present study aimed to identify if the use of a high dose of RSV could have a synergistic effect on PAC at a lower dose in MPM. Several studies have reported that RSV could inhibit the growth of cancer cells *in vitro* when present at a high concentration of above 50 µM or when used in combination with other anticancer drugs [29-32]. RSV at 62.5 µM didn't cause cytotoxic effects on normal kidney cells HEK 293 in preliminary study.

The main findings of this study indicated that at a low dose of 3 µM PAC and RSV at 62.5 µM, more cell death was observed than with individual PAC or RSV alone. Decreased in cell viabilities,

induction of ROS formation, increased in pro-apoptotic caspases -3, -7, -8, -9, decreased in expressions of MEK -1, -2, -3, -4, decreased in cell cycle regulatory proteins, and decreased in PD-L1 and EGFR expression demonstrate how the combination of PAC and RSV could inhibit MPM cell growth from severe metastatic cancer. In a study conducted by Chae et al., the impact of quercetin (Qu), a compound found in plants, was examined. They found that Qu triggered the activation of Bid and caspase-3, while simultaneously reducing Bcl-xL levels and increasing Bax levels in MSTO-211H cells. Additionally, they observed a decrease in cyclin D1 expression mediated through the Sp1 gene [33]. These results closely parallel to my findings, where I also observed a decrease in Bcl-xL and an increase in Bax levels, as well as a reduction in cyclin D1 expression. These changes are critical in inhibiting the proliferation and survival of MSTO cells, underscoring the importance of targeting these pathways in cancer therapy. A study used RSV 15 µM and clofarabine 40 nM synergistically caused apoptosis signal via p53-dependent pathway in MSTO cells as well [34].

The combination of RSV and PAC reduced MSTO-211H cell viability to a greater extent than treatment with RSV or PAC alone. An increase in nuclear condensation of apoptotic cells stained with Hoechst 33342 was observed at a higher level than with individual RSV or PAC treatment. Additionally, nuclear-ID red/green cell staining data confirmed that more cell deaths were observed in MSTO-211H cells treated with combined PAC and RSV treatment.

Evidence suggests that cancer cells generate more intracellular ROS than normal cells [35]. Increased ROS levels in MPM are associated with the modulation of several key signaling proteins involved in DNA damage, changes in tumor suppression proteins, apoptosis, and cell cycle regulation and differentiation [36, 37]. Activation of AIF-1, a tumor suppressor, and initiator of caspases -8 and -9 forming the apoptosome, which further activates executioner caspases -3 and -7 during cell death. This study shows for the first time that the combination of PAC and RSV significantly initiates the apoptotic cascade through activation of AIF-1 and enhanced expression of caspases -3, -7, -8, and -9.

ROS also plays a crucial role in modulating the pro-apoptotic protein Bax and the anti-apoptotic protein Bcl2. Slight changed in the ratio of Bax/Bcl2 were identified in cells treated with RSV alone or combination of RSV and PA versus control. The modulation of Bax/Bcl2 is preceded by the collapse of the mitochondrial membrane potential, which has been associated with the initiation of the caspase cascade leading to cell death [38]. The reduction in mitochondrial membrane potential, which causes the release of cytochrome C into the cytosol, further signifies apoptotic events [39]. The expression of cytochrome C was significantly higher in cells treated with the combination of PAC and RSV. Furthermore, an increase in ROS accumulation was confirmed by the H2DCFDA staining assay, indicating a synergistic effect of PAC and RSV. Rhodamine 123 staining also confirmed a reduction in mitochondrial membrane potential in the combined PAC and RSV treatment group.

The combination of RSV and PAC also caused a decrease in MEK-1, -2, -3, -4 expressions. MAPKs are Ser/Thr kinases that play an important role in cellular responses such as proliferation, differentiation, transformation, and apoptosis [40]. Chemotherapeutic agents that target the aberrant cell signaling of MAPKs and their active phosphorylated forms of MEK-1, -2, -3, and -4 provide promising therapeutic benefits.

The combination of RSV and PAC also had a profound effect on inhibiting proteins involved in cell cycle regulation. Several cells cycle regulatory proteins such as cyclin-dependent kinases, cyclin D1, along with Cyclin C and E, have been shown to inhibit the G1 phase, while cyclin B1 inhibits the G2/M phase [41-43]. Inhibition of cyclin B1 and D1 was observed in the combination of PAC and

RSV. Additionally, CDK2, which inhibited G1/S phase, and CDK7, which inhibited the G2 phase, were also noted in the combination of PAC and RSV. This study showed significant downregulation of cell cycle proteins at different phases of the cell cycle, which could provide promising future treatments for MPM.

Cancer cells have been known to secrete epidermal growth factor (EGF) and other growth factors to activate receptor tyrosine kinases, leading to the phosphorylation of tyrosine residues, which further causes unlimited mitotic proliferation of cancer cells [44, 45]. EGFR is commonly upregulated in metastatic colorectal, breast, or non-small cell lung cancers [46-48]. As a multifunctional cell growth regulator that can stimulate cell proliferation, promote the growth and differentiation of epidermal cells and other tissue cells, and stimulate the malignant transformation of cells, targeting EGFR could provide a beneficial effect in MPM treatment [44]. In this study, the combination of PAC and RSV inhibited the expression of EGFR more than individual PAC or RSV alone. Additionally, EGFR has also been known to activate downstream cell signaling such as cyclin D1 and CDK4/6 involved in cell cycle progression [46, 47]. Therefore, targeting the inhibition of EGFR can serve as an important biomarker and a potentially successful treatment for MPM.

Cancer cells have also been shown to be sensitive to immunotherapy such as checkpoint inhibitors that function as negative regulators of programmed death ligand 1 (PDL-1) [49-52]. PDL1 is a glycoprotein molecule that is expressed in various immune cells and cancer cells such as hepatocellular carcinoma, colorectal cancer, breast cancer, lung cancer, pancreatic cancer, and MPM [49-53]. A recent meta-analysis study assessing the potential prognostic significance of PDL-1 expression in MPM concluded that high expression of PDL-1 significantly can be used as a prognostic tool for poor outcomes in patients with MPM [53]. This study showed that the combination of PAC and RSV, which decreased PDL-1, may be used as a treatment option in the future. The proposed diagram shows mechanism of action of combine PAC and RSV in causing cell death and cell cycle arrest in PMP [Figure 12].

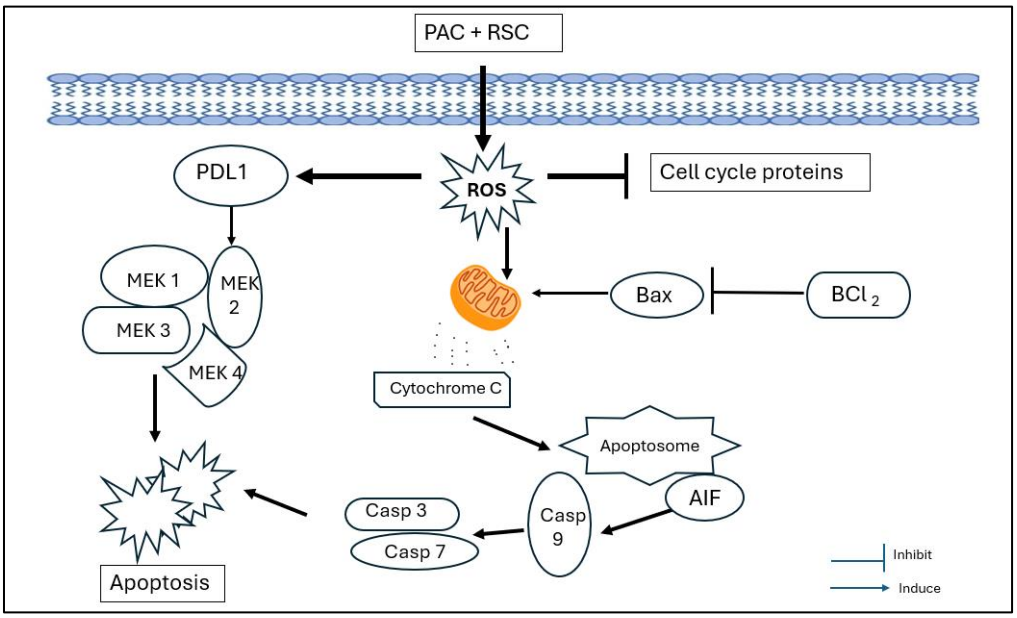

Figure 12 Schematic diagram representing the apoptosis signaling proteins and cell cycle arrest when MSTO cells were treated with PAC and RSV combination.

5. Conclusions

Malignant pleural mesothelioma (MPM) is a highly aggressive cancer with limited treatment options, typically associated with poor prognosis. Standard therapies, such as surgery, chemotherapy, and radiation, often yield suboptimal results, highlighting the need for novel therapeutic strategies. The combination of Paclitaxel (PAC), a well-established chemotherapeutic agent, and Resveratrol (RSV), a natural antioxidant with anticancer properties, has demonstrated synergistic cytotoxic effects in vitro, suggesting a potential new avenue for MPM treatment.

In this preclinical study, the PAC-RSV combination led to a significant increase in cancer cell death, primarily through the inhibition of cell cycle proteins and induction of apoptosis via caspase-3, -7, -8, and -9 pathways. Furthermore, this combination inhibited key oncogenic signaling molecules such as MEK1-4, PDL1, and EGFR, which are frequently overexpressed in MPM. By blocking these pathways, the PAC-RSV combination not only limits cancer cell proliferation but also enhances immune recognition and promotes apoptosis, effectively reducing tumor growth.

Given the limited treatment options available for MPM, the findings from this study provide a promising foundation for advancing the PAC-RSV combination into clinical trials. The ability of these agents to target multiple mechanisms of cancer progression — including cell cycle arrest, immune checkpoint inhibition, and apoptosis induction — offers a multifaceted approach that could enhance treatment efficacy and overcome resistance to conventional therapies. If validated in clinical trials, this combination therapy could become a novel, effective treatment option for MPM patients, improving both survival rates and quality of life.

The results from this study underscore the potential for PAC and RSV to be integrated into existing therapeutic regimens or developed as a standalone treatment for MPM, ultimately providing hope for patients with this challenging disease.

Author Contributions

LLB: conceptualization, investigation, writing, original draft, review, editing, submitting.

Funding

Union University.

Competing Interests

The author has declared that no competing interests exist.

Data Availability Statement

The data are available from the corresponding author upon reasonable request.

References

1. Karunakaran KB, Yanamala N, Boyce G. Malignant pleural mesothelioma interactions with 364 novel protein-protein interactions. Cancer. 2021; 13: 1660.
2. Mutti L, Peikert L, Robinson BW, Scherpereel A, Tsao AS, de Perrot M, et al. Scientific advances, and new frontiers in mesothelioma therapeutics. J Thorac Oncol. 2018; 13: 1269-1283.

3. Roe OD, Stella GM. Malignant pleural mesothelioma: History, controversy and future of a man made epidemic. Eur Respir Rev. 2015; 24: 115-131.
4. Kuryk L, Rodella G, Staniszewska M. Novel insights into mesothelioma therapy: Emerging avenues and prospects. Front Oncol. 2022; 12: 916839.
5. Carbone M, Baris YI, Bertino P, Miller A. Erionite exposure in North Dakota and Turkish villages with mesothelioma. Proc Natl Acad Sci U S A. 2021; 108: 13618-13623.
6. Baumann F, Buck BJ, Metcalf RV. The presence of asbestos in the natural environment is likely related to mesothelioma in young individuals and women from Southern Nevada. J Thorac Oncol. 2015; 10: 731-737.
7. Callis L. EPA makes 'historic' ruling to ban hazardous material: "A symbol of how [the] law can and must be used [Internet]. The Cool Down Company; 2024 [cited date 2024 April 13]. Available from: https://www.thecooldown.com/green-business/asbestos-ban-epa-chrysotile-us/.
8. Peto J, Decarli A, La Vecchia C, Levi F, Negri E. The European mesothelioma epidemic. Br J Cancer. 1999; 79: 666-672.
9. Fennell DA, Gaudino G, O'Byrne KJ. Advances in the systemic therapy of malignant pleural mesothelioma. Nat Clin Pract Oncol. 2008; 5: 136-147.
10. Scherpereel A, Astoul P, Baas P, Berghmans T, Clayson P, Dienemann H. Guidelines of the European Respiratory Society and the European Society of Thoracic Surgeons for the management of malignant pleural mesothelioma. Eur Respir J. 2010; 35: 479-495.
11. Broggi G, Angelico G, Filetti V. Immunohistochemical expression of serine and arginine-rich splicing factor 1 (SRSF1) in fluoro-edenite-induced malignant mesothelioma: A preliminary study. Int J Environ Res Public Health. 2021; 18: 6249.
12. Rapisarda V, Broggi G, Caltabiano R. ATG7 immunohistochemical expression in malignant pleural mesothelioma. A preliminary report. Histopathology. 2021; 36: 1301-1308.
13. Piggott LM, Hayes C, Greene J, Fitzgerald DB. Malignant pleural disease. Breath. 2023; 19: 230145.
14. Creaney J, Robinson BW. Malignant mesothelioma biomarkers - from discovery to use in clinical practice for diagnosis, monitoring, screening, and treatment. Chest. 2017; 152: 143-149.
15. Ceresoli GL, Zucali PA, Favaretto AG. Phase II study of pemetrexed plus carboplatin in malignant pleural mesothelioma. J Clin Oncol. 2006; 24: 1443-1448.
16. Tsao AS, Pass HI, Rimmer A, Mansfield AS. New era for malignant pleural mesothelioma: Updates on therapeutic options. J Clin Oncol. 2022; 40: 681-692.
17. Baas P, Scherpereel A, Nowak AK. First-line nivolumab plus ipilimumab in unresectable malignant pleural mesothelioma (Checkmate 743): A multicenter randomized, open-label, phase 3 trial. Lancet. 2021; 397: 375-386.
18. Schulte JJ, Husain AN. Update on the pathologic diagnosis of malignant mesothelioma. Transl Lung Cancer Res. 2020; 9: 917-923.
19. Kindler HL, Ismalia N, Armato III SG, Bueno R, Hesdorgger M, Jahan T. Treatment of malignant pleural mesothelioma: American Society of Clinical Oncology Clinical Practice Guideline. J Clin Oncol. 2018; 36: 1343-1373.
20. Meng Z, Lv Q, Lu J, Yao H, Lv X, Jiang F, et al. Prodrug strategies for paclitaxel. Int J Mol Sci. 2016; 17: 796.

21. De Furia MD. Paclitaxel (Taxol): A new natural product with major anticancer activity. Phytomedicine. 1997; 4: 273-282.
22. Weaver BA. How Taxol/paclitaxel kills cancer cells. Mol Biol Cell. 2014; 25: 2677-2681.
23. Shi Y, Yang S, Troup X. Resveratrol induces apoptosis in breast cancers by E2F1-mediated upregulation of ASPPI. Oncol Rep. 2011; 25: 1713-1719.
24. Lee YJ, Lee YK, Lee SH. Resveratrol and clofarabine induces a preferential apoptosis-activating effect on malignant mesothelioma cells by Mcl-1 down regulation and caspase-3 activation. BMB Rep. 2015; 48: 166-171.
25. Mondal A, Bennett LL. Resveratrol enhances the efficacy of sorafenib mediated apoptosis in human breast cancer MCF7 cells through ROS, cell cycle inhibition, caspase 3 and PARP cleavage. Biomed Pharmacotherapy. 2016; 84: 1906-1914.
26. Bennett LL, Mondal A. Curcumin and afatinib synergistically inhibit growth of human osteosarcoma cells by inhibition of matrix Metallo proteinase, mitogen activated kinase 1-4, and reactive oxygen species. J Pharm Drug Dev. 2021; 3: 2.
27. Vichai V, Kirtikara K. Sulforhodamine B colorimetric assay for cytotoxicity screening. Nat Protoc. 2006; 1: 1112-1116.
28. Fukui M, Yamabe N, Zhu BT. Resveratrol attenuates the anticancer efficacy of paclitaxel in human breast cancer cells in vitro and in vivo. Eur J Cancer. 2010; 46: 1882-1891.
29. Pozo-GE, Merino JM, Mulero-Navarro S, Lorenzo-Benayas J, Centeno F, Alvarez-Barrientos A, et al. Resveratrol-induced apoptosis in MCF-7 human breast cancer cells involves a caspase-independent mechanisms with downregulation of Bcl-2 and NF-kappa B. Int J Cancer. 2005; 115: 74-84.
30. Aziz MH, Nihal M, Fu VX. Resveratrol-caused apoptosis of human prostate carcinoma LNCaP cells in mediated via modulation of phosphatidylinositol 3'-kinase/Akt pathway and BCl-2 family proteins. Mol Cancer Ther. 2006; 5: 1335-1341.
31. Gill C, Walsh SE, Morrissey C, Fitpatrick JM, Watson RW. Resveratrol sensitizes androgen-independent prostate cancer cells to death receptor mediated apoptosis through multiple mechanisms. Prostate. 2007; 67: 1641-1653.
32. Alkhalaf M. Resveratrol-induced growth inhibition in MDA-MB-231 breast cancer cells is associated with mitogen-activated protein kinase signaling and protein translation. Eur J Cancer Prev. 2007; 16: 334-341.
33. Chae J-Il, Cho JH, Lee Kyung-Ae. Role of transcription factor Sp1 in the quercetin-mediated inhibitory effect on human malignant pleural mesothelioma. Int J Mol Med. 2012; 30: 21-27.
34. Lee YJ, Park IS, Lee YJ, Shim JH, Ch MK, Nam HS. Resveratrol contributes to chemosensitivity of malignant mesothelioma cells with activation of p53. Food Chem Toxicol. 2014; 63: 153-160.
35. Simon HU, Haj-Yehia A, Levi-Schaffer F. Role of reactive oxygen species (ROS) in apoptosis induction. Apoptosis. 2000; 5: 415-418.
36. Mates JM, Sanchez-Jimenez FM. Role of reactive oxygen species in apoptosis: Implications for cancer therapy. Int J Biochem Cell Biol. 2000; 32: 157-170.
37. Zhang T, Brazhnik P, Tyson JJ. Exploring mechanisms of the DNA-damage response: p53 pulses and their possible relevance to apoptosis. Cell Cycle. 2007; 6: 85-94.
38. Penninger JM, Kroemer G. Mitochondria, AIF and caspases-rivaling for cell death. Nat Cell Biol. 2003; 5: 97-99.

39. Yang Y, Liu X, Bhalla K. Prevention of apoptosis by Bcl-2 release cytochrome c from mitochondria blocked. Science. 1997; 275: 1129-1132.
40. Li Y, Dong Q, Cui Y. Synergistic inhibition of MEK and reciprocal feedback networks for targeted intervention in malignancy. Cancer Biol Med. 2019; 16: 415-434.
41. Otto T, Sicinski P. Cell cycle proteins as promising targets in cancer therapy. Nat Rev Cancer. 2017; 17: 93-115.
42. Choi YJ, LI A, Hydbring P, Sanda T, Stefano J, Christie AL. The requirement for cyclin D1 function in tumor maintenance. Cancer Cell. 2012; 22: 438-451.
43. Okuda M, Horn HF, Tarapore P. Nucleoplasm B23 is a target of CDk2/cyclin E in centrosome duplication. Cell. 2000; 103: 127-140.
44. Chen J, Chen J, LV X. Epidermal growth factor in exhaled breath condensate as diagnostic method for non-small cell lung cancer. Technol Cancer Res Treat. 2019; 218: 1533033819872271.
45. Brueck WM, Schoeber A, Wirtz RM. Increased vascular-endothelial growth factor (VEGF) tumor expression and response to epidermal growth factor receptor (EGF-R) inhibitor erlotinib in non-small cell lung cancer (NSCLC). J Thorac Oncol. 2008; 23: 314-316.
46. Wee P, Wang Z. Epidermal growth factor receptor cell proliferation signaling pathways. Cancers. 2017; 9: 52.
47. Chen SJ, Luan J, Zhang HS, Ruan CP, Xu XY, Li QQ. EGFR-mediated G1/S transition contributes to the multidrug resistance in breast cancer cells. Mol Biol Rep. 2012; 39: 5465-5471.
48. Bai Y, Chen A, Hou L. PD-L1 expression and its effect on clinical outcomes of EGFR-mutant NSCLS patients treated with EGFR-TKIs. Cancer Biol Med. 2018; 15: 434-442.
49. Jin L, Gu W, Li X. PD-L1 and prognosis in patients with malignant pleural mesothelioma: A meta-analysis and bioinformatics study. Ther Adv Med Oncol. 2020; 12: 1758835920962362.
50. Li XS, Li JW, Li H, Jiang T. Prognostic value of programmed cell death ligand 1 (PD-L1) for hepatocellular carcinoma: A meta-analysis. Biosci Rep. 2020; 40: BSR20200459.
51. Li SC, Chen L, Jiang J. Role of programmed cell death ligand-1 expression on prognostic and overall survival of breast cancer: A systematic review and meta-analysis. Medicine. 2019; 98: e15201.
52. Li H, Xu Y, Wan B, Song Y, Zhan P, Hu Y. The clinic pathological and prognostic significance of PD-L1 expression assessed by immunohistochemistry in lung cancer: A meta-analysis of 50 studies with 11,383 patients. Transl Lung Cancer Res. 2019; 8: 429-449.
53. Hu Y, Chen W, Yan Z, Ma Z, Fangshi Z, Jiege H. Prognostic value of PD-L1 expression in patients with pancreatic cancer: A PRISMA-compliant meta-analysis. Medicine. 2019; 98: e14006.